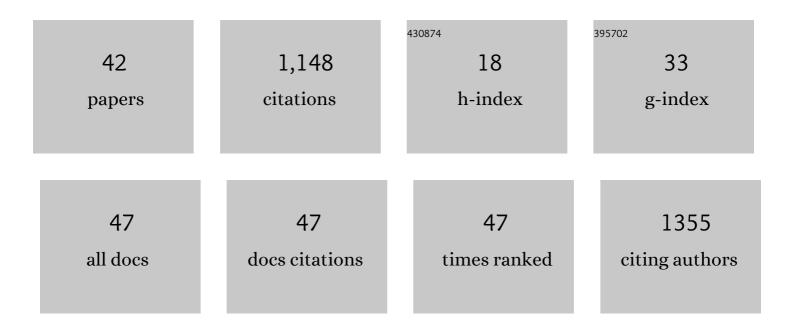
Hong Sun

List of Publications by Year in descending order

Source: https://exaly.com/author-pdf/2564663/publications.pdf Version: 2024-02-01



HONC SUN

#	Article	IF	CITATIONS
1	Microstructure and mechanical properties of Cr films deposited with different peak powers by high-power impulse magnetron sputtering. Rare Metals, 2023, 42, 327-335.	7.1	2
2	Highâ€Throughput DNA Tensioner Platform for Interrogating Mechanical Heterogeneity of Single Living Cells. Small, 2022, 18, e2106196.	10.0	15
3	<i>Lactobacillus paracasei</i> 24 Attenuates Lipid Accumulation in High-Fat Diet-Induced Obese Mice by Regulating the Gut Microbiota. Journal of Agricultural and Food Chemistry, 2022, 70, 4631-4643.	5.2	31
4	Companion-Probe & Race platform for interrogating nuclear protein and migration of living cells. Biosensors and Bioelectronics, 2022, 210, 114281.	10.1	4
5	MnOx location on MnOx-ZSM-5 to influence the catalytic activity for selective catalytic reduction of NOx by NH3. Applied Catalysis A: General, 2021, 617, 118128.	4.3	27
6	Detection of chlorophyll fluorescence parameters of potato leaves based on continuous wavelet transform and spectral analysis. Spectrochimica Acta - Part A: Molecular and Biomolecular Spectroscopy, 2021, 259, 119768.	3.9	28
7	Analysis of Chlorophyll Concentration in Potato Crop by Coupling Continuous Wavelet Transform and Spectral Variable Optimization. Remote Sensing, 2020, 12, 2826.	4.0	25
8	Detection of chlorophyll content in growth potato based on spectral variable analysis. Spectroscopy Letters, 2020, 53, 476-488.	1.0	15
9	Application of Color Featuring and Deep Learning in Maize Plant Detection. Remote Sensing, 2020, 12, 2229.	4.0	18
10	Growth Stages Classification of Potato Crop Based on Analysis of Spectral Response and Variables Optimization. Sensors, 2020, 20, 3995.	3.8	27
11	Dynamic Influence Elimination and Chlorophyll Content Diagnosis of Maize Using UAV Spectral Imagery. Remote Sensing, 2020, 12, 2650.	4.0	29
12	Detection of Canopy Chlorophyll Content of Corn Based on Continuous Wavelet Transform Analysis. Remote Sensing, 2020, 12, 2741.	4.0	32
13	Optimal fertigation for high yield and fruit quality of greenhouse strawberry. PLoS ONE, 2020, 15, e0224588.	2.5	10
14	Novel metal-organic framework supported manganese oxides for the selective catalytic reduction of NOx with NH3: Promotional role of the support. Journal of Hazardous Materials, 2019, 380, 120800.	12.4	36
15	Effects of Cantharidin and Norcantharidin on Larval Feeding and Adult Oviposition Preferences of the Diamondback Moth (Lepidoptera: Plutellidae). Journal of Economic Entomology, 2019, 112, 1634-1637.	1.8	6
16	Engineering phytosterol transport system in Mycobacterium sp. strain MS136 enhances production of 9α-hydroxy-4-androstene-3,17-dione. Biotechnology Letters, 2018, 40, 673-678.	2.2	15
17	Catalytic Formation of Nitric Oxide Mediated by Ti–Cu Coatings Provides Multifunctional Interfaces for Cardiovascular Applications. Advanced Materials Interfaces, 2018, 5, 1701487.	3.7	12
18	Characterization of Ti-Cu Films Deposited by HPPMS and Effect on NO Catalytic Release and Platelet Adhesion Behavior. Journal Wuhan University of Technology, Materials Science Edition, 2018, 33, 505-511.	1.0	1

Hong Sun

#	Article	IF	CITATIONS
19	Research on Cloud Computing Modeling Based on Fusion Difference Method and Self-Adaptive Threshold Segmentation. International Journal of Pattern Recognition and Artificial Intelligence, 2018, 32, 1859010.	1.2	9
20	Self-Assembled Magnetic Viruslike Particles for Encapsulation and Delivery of Deoxyribonucleic Acid. Langmuir, 2018, 34, 7171-7179.	3.5	12
21	Tailoring of TiO2 films by H2SO4 treatment and UV irradiation to improve anticoagulant ability and endothelial cell compatibility. Colloids and Surfaces B: Biointerfaces, 2017, 155, 314-322.	5.0	13
22	Functional polymorphisms in the promoter region of miR-17-92 cluster are associated with a decreased risk of colorectal cancer. Oncotarget, 2017, 8, 82531-82540.	1.8	16
23	Self-patterning porous films of giant vesicles of {Mo 72 Fe 30 }(DODMA) 3 complexes as frameworks. Advances in Colloid and Interface Science, 2016, 235, 14-22.	14.7	13
24	A green synthesis of "naked―Pt and PtPd catalysts for highly efficient methanol electrooxidation. RSC Advances, 2016, 6, 56083-56090.	3.6	16
25	Enhanced catalytic activity over MIL-100(Fe) loaded ceria catalysts for the selective catalytic reduction of NO x with NH 3 at low temperature. Journal of Hazardous Materials, 2016, 301, 512-521.	12.4	68
26	A polymorphism rs4705341 in the flanking region of miR-143/145 predicts risk and prognosis of colorectal cancer. Oncotarget, 2016, 7, 62084-62090.	1.8	13
27	Ag2S/CdS/TiO2 Nanotube Array Films with High Photocurrent Density by Spotting Sample Method. Nanoscale Research Letters, 2015, 10, 382.	5.7	14
28	Catalytic ozonation of reactive red X-3B in aqueous solution under low pressure: decolorization and OH· generation. Frontiers of Environmental Science and Engineering, 2015, 9, 591-595.	6.0	3
29	A portable soil nitrogen detector based on NIRS. Precision Agriculture, 2014, 15, 3-16.	6.0	32
30	The Direct Synthesis of Graphene on a Gallium Nitride Substrate. Chemical Vapor Deposition, 2014, 20, 125-129.	1.3	10
31	Porous metal–organic framework MIL-100(Fe) as an efficient catalyst for the selective catalytic reduction of NO _x with NH ₃ . RSC Advances, 2014, 4, 48912-48919.	3.6	80
32	Carbon-Doped Titanium Oxide Films by DC Reactive Magnetron Sputtering Using CO2 and O2 as Reactive Gas. Acta Metallurgica Sinica (English Letters), 2014, 27, 239-244.	2.9	9
33	The effect of full/partial UV-irradiation of TiO 2 films on altering the behavior of fibrinogen and platelets. Colloids and Surfaces B: Biointerfaces, 2014, 122, 709-718.	5.0	21
34	Effect of the total saponins of Aralia elata (Miq) Seem on cardiac contractile function and intracellular calcium cycling regulation. Journal of Ethnopharmacology, 2014, 155, 240-247.	4.1	59
35	Aconitine-induced Ca2+ overload causes arrhythmia and triggers apoptosis through p38 MAPK signaling pathway in rats. Toxicology and Applied Pharmacology, 2014, 279, 8-22.	2.8	78
36	Electrochemical in situ regeneration of granular activated carbon using a three-dimensional reactor. Journal of Environmental Sciences, 2013, 25, S77-S79.	6.1	15

Hong Sun

3

#	Article	IF	CITATIONS
37	Microstructure and Platelet Adhesion Behavior of Titanium Oxide Films Synthesized by Reactive High-Power Pulse Magnetron Sputtering. IEEE Transactions on Plasma Science, 2013, 41, 1837-1843.	1.3	6
38	Indentation strength of ultraincompressible rhenium boride, carbide, and nitride from first-principles calculations. Physical Review B, 2012, 86, .	3.2	58
39	Unexpectedly low indentation strength of WB <mmi:math xmlns:mml="http://www.w3.org/1998/Math/MathML" display="inline"><mml:msub><mml:mrow /><mml:mn>3</mml:mn></mml:mrow </mml:msub>and MoB<mml:math xmlns:mml="http://www.w3.org/1998/Math/MathML" display="inline"><mml:msub><mml:mrow /><mml:mn>3</mml:mn></mml:mrow </mml:msub>from first principles. Physical Review B, 2012, 86,</mml:math </mmi:math 	3.2	49
40	Ideal strength and structural instability of aluminum at finite temperatures. Physical Review B, 2012, 86, 86, 86, . 86, .	3.2	24
41	Enhancement of Catalytic Activity Over the Iron-Modified Ce/TiO ₂ Catalyst for Selective Catalytic Reduction of NO _{<i>x</i>} with Ammonia. Journal of Physical Chemistry C, 2012, 116, 25319-25327.	3.1	189

42 Evaluation of maize growth by ground based multi-spectral image., 2011, , .